

## The Application of Waste Float Glass, Recycled in Structural Beams made with the Glass Casting Method

Yu, R.; Bristogianni, T.; Veer, F.A.; Nijssse, R.

**DOI**

[10.7480/cgc.7.4775](https://doi.org/10.7480/cgc.7.4775)

**Publication date**

2020

**Document Version**

Final published version

**Published in**

Challenging Glass Conference

**Citation (APA)**

Yu, R., Bristogianni, T., Veer, F. A., & Nijssse, R. (2020). The Application of Waste Float Glass, Recycled in Structural Beams made with the Glass Casting Method. In C. Louter, F. Bos, & J. Belis (Eds.), *Challenging Glass Conference: Conference on Architectural and Structural Applications of Glass, CGC 7 TU Delft OPEN* Publishing. <https://doi.org/10.7480/cgc.7.4775>

**Important note**

To cite this publication, please use the final published version (if applicable).  
Please check the document version above.

**Copyright**

Other than for strictly personal use, it is not permitted to download, forward or distribute the text or part of it, without the consent of the author(s) and/or copyright holder(s), unless the work is under an open content license such as Creative Commons.

**Takedown policy**

Please contact us and provide details if you believe this document breaches copyrights.  
We will remove access to the work immediately and investigate your claim.

# The Application of Waste Float Glass, Recycled in Structural Beams made with the Glass Casting Method.

Rong Yu <sup>a</sup>, Telesilla Bristogianni <sup>a</sup>, Fred A. Veer <sup>b</sup>, Rob Nijse <sup>a, b</sup>

<sup>a</sup> TU Delft, Faculty of Civil Engineering and Geosciences, The Netherlands, [Rong.Yu@tudelft.nl](mailto:Rong.Yu@tudelft.nl)

<sup>b</sup> TU Delft, Faculty of Architecture and the Built Environment, The Netherlands

It is not obvious to talk about glass recycling when we realize that a mature recycling procedure for glass bottles is already working well. However, apart from glass bottles, unfortunately that a large amount of glass will disappear into landfill. This large quantity of unrecycled glass indicates that there is a large potential in upgrading the glass recycling process. In the field of architecture, we see a fast-growing interest in using glass, also for structures. The glass bricks of Crystal Houses in Amsterdam are a good illustration. Aiming at maximizing the recyclability of glass, this paper focus on the structural use of the glass components made from recycled glass through kiln casting method. An overview of the existing glass recycling industry is given at the beginning, followed by a discussion of glass type to be recycled. After this the experimental process of the glass recycling is introduced, which uses coated float glass with tints as the basic material to be recycled. Following this, a further exploration in three structural properties of the recycled products is conducted, namely: Young's modulus, coefficient of thermal expansion and the fracture strength, with mechanical experiments. Finally, the test results are analyzed together with the chemical composition of the recycled products, which is derived from X-ray fluorescence (XRF) analysis. The result contains the value of mechanical properties and it evaluates the possibility of the structural use as a recycled-float-glass beam. In the end of this paper, the future possibility and feasibility in structural application of recycling waste float glass are discussed.

**Keywords:** Glass recycling, Cast glass components, Structural glass

## 1. Introduction

### 1.1. The current situation and potential of glass recycling

There are great potential in glass recycling industry, not only because of its substantial high degree of recyclability, but also because its outstanding behavior both as a structural component and architectural component. According to the existing glass recycling industry, the type of glass wastes can be briefly divided into three parts, classified by their disposition. First, the post-consumer containers, such as glass bottles or jars, is widely known by the public as recycling without changing their physical form. There are matured recycling industry lines from collection, industrial treatment to reuse and resale it. Second, the waste glass from manufacture factory from production line, such as flat glass, is another part of waste glass. These industry waste glass mainly recycled by the factory itself, through crushing into glass cullet following by remelting as part of raw material. However, the category of glass waste is way more than two types above, for instance, the waste glass from electronical products (i.e. the cathode ray tubes for computer or TV screens and the liquid crystal display glass), the glassware from daily life (i.e. decorative glass, ceramic glass or optical glass), or the fire-resistant glass (i.e. the glass from kitchenware or laboratory) (Silva et al., 2017). Here the author concludes this unsolved waste glass as the third category. Due to the contamination (such as metal, plastic or paper label), lamination, coating or adhesives, a great difficulties seats in purifying these waste glass. Moreover, the difference in remelting process also varies from different types of glass, which lead to impossibility in recycling glass mixtures. Nowadays, the majority of these glass, including the waste glass which eliminated from the glass manufactory because of the low quality, is down recycling into landfilled or construction products (Bristogianni et al., 2018).

### 1.2. The feasibility of recycled glass products

For centuries, glass as a material is becoming more and more essential in science and technology, as well as peoples' daily life. It is widely used in optical equipment, light industry and especially the architectural field. Whereas, the structural utilization of glass has been developed by engineers in recently decades. Growing with the understanding of glass material properties, the strength in strong compression resistance of glass have been noticed by engineers. Integrating with the completely recyclability and high transparency, the glass is able to be the superior compressive material compare to concrete or bricks. At the first phases, structural glass products were expressed as flat components, which is mainly the results of limitations from manufactory technology. However, with the adoption of casting method, the 3D structural glass components can be realized. Through this solid glass component, a self-loading even load-bearing application can be obtained under structural employment, such as Crystal Houses in Amsterdam

(Oikonomopoulou et al., 2018). Integrating with the glass recycling, the casting technology is also an applicable method to recycle different glasses owing to the accessibility of material and temperature change.

To take the advantage of recyclability and load-bearing capacity of glass, a concept of structural glass beams made of waste glass through casting method has been developed. This paper aims to evaluating the applicability of recycled-glass beam, by studies on chemical composition change in recycling and mechanical properties.

## 2. Experiment and results

### 2.1. Selection of material and methodology

- Selection of the recycled material:

Among the down-recycled glass types as mentioned above, there is a great proportion of float glass. Thus, this paper selected the float glass, mainly used for architectural purpose, as aiming resource. The architectural float glass can be categorized as soda-lime-silicate glass, which includes approximately 72% to 74% silicon dioxide and 12% to 15% sodium oxide as the main chemical composition (Vieitez et al., 2011). Generally speaking, there are four main obstacles rest in the recycling of float glass, conclude as laminations (such as PVB or EVA layers used between the float glass panels), adhesives (the binders which makes strong connections between float glasses or bonding glass with other materials), tints (the durable color made by changing of the chemical formulations of glass), and coatings (a layer on top of the glass aiming at affect the transmission, assisted in improving glass appearance and surface condition). The recent glass recycling industry have working lines specially remove laminations and adhesives, which are usually manual work. In the meantime, considering the amount of metal oxides which producing the tints is relatively low, the structural influence of glass tints will not be included in this paper. Thus, the coatings will be considered as the only influence factor in this paper.

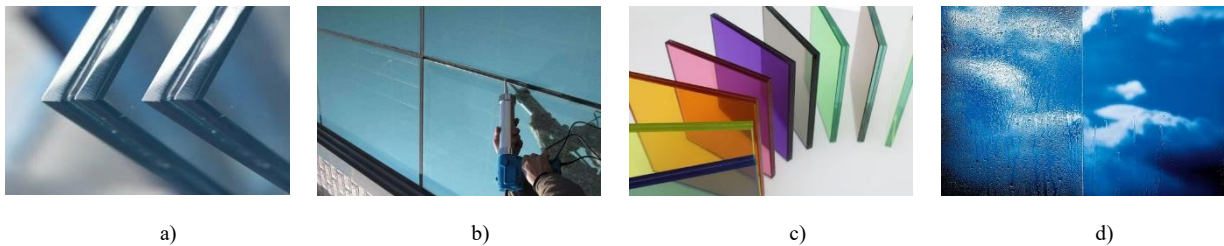


Fig. 1a), b), c) and d) Illustrations of glass lamination, adhesives, tints and coatings.

Referring to Pilkington coating technology (Coating Technology - Processes, n.d.), there are three approaches to apply coatings on float glass. The simplest way called Plasma Vapour Deposition (PVD), in which the gas plasma is sputtered into the target surface. Besides, with the development of magnetrons, coatings can be sputtered to glass surface in various directions with higher rates, which is called Magnetron Sputtering Process. In these two approaches, coatings only attached to the target surface without any chemical reaction, thus, they are known as “soft coating”. On the contrary, “hard coating”, a coating process contains chemical bond rupture and formation exists. It is called as Chemical Vapour Deposition (CVD), in which the gaseous mixture will be introduced to the target float glass, under a high temperature ranging from 482 degrees to 732 degrees. The hard coating is the outcome of pyrolytic reaction, indicating the strong chemical bond connection (Glass Coating Technology Comparison | Stewart Engineers, n.d.).



Fig. 2a), b) c) and d) The glass samples from Pilkington, from a) to d) is float glass, light soft coating glass, dark soft coating glass and hard coating glass.

To simplify the category, the samples are distinguished by hard coating and soft coating in this experiment. Supporting from Pilkington, four kinds of glass samples are provided, shown in figure 2, including normal float glass, soft coating with light green tints, soft coating glass with dark green tints and hard coating glass. All glass samples are coated only on one side. Based on the manufacture process of float glass, there will be a tin bath side in all float glass. Thus, before






*The Application of Waste Float Glass, Recycled in Structural Beams made with the Glass Casting Method.*

the experiment, not only the coated side, but also the tin side are recognized, a detailed differentiation will be obtained through XRF test.

● Casting methodology:

In order to satisfy the requirement for the various mechanical test, samples with two different dimensions are provided, listing as below:

Table 1: Illustration of all the relative samples.

Dimension 1		Dimension 2			
	Sample 1	Sample 2	Sample 3	Sample 4	Sample 5 - 10
Original material	Normal float glass	Light soft coating glass	Dark soft coating glass	Hard coating glass	Soft coating 1 glass, soft coating 2 glass and hard coating glass in the ratio of 3:3:2
Status before casting					
Length [cm]	15.5				~36
Width [cm]	3.5				~3.6
Thickness [cm]	4.5				1.2
Aiming tests	XRF test, Young's modulus test, CTE test.				Fracture strength test

Based on the experimental conditions, a kiln casting method was chosen, which containing casting steps as: original model preparation, rubber mould production, wax model fabrication, crystal-cast mould production and furnacing. With kiln casting, the waste float glass will be carefully cleaned before being placed freely in crystalcast mould (crystalcast M248, consists of cristobalite, quartz and gypsum). On account of the existing float glass types, four samples were prepared separately shown as sample 1 to 4. To obtain the bending test, another five samples with different dimension prepared with the mixture of coated float glass, the details also shown in the table above. Afterwards, the whole unit will be put into the oven for furnacing.

Regarding to the types of glass samples from Pilkington, the estimated melting temperature ranging from 900 degrees to 1250 degrees (Bristogianni et al., 2018). Considering the result from the previous experiment, in which the float glass was not completely melted at 900 degrees, obvious lumps were fused together in that recycled sample. Therefore, to maximizing the homogeneity of the end products with a conceivable minimum energy consumption, the aim temperature was set as 1100 degrees. Restricted by the source delivery, the hard coating samples are recycled separately. The firing schedule for these two batches sharing the same highest temperature with similar firing process, as well as the third firing for the sample 5 -10, shown in the figure 3.

The firing process is concluded as five steps, shown as heating period, casting period, quenching period, annealing period and final cooling period in the chart. A difference seats in the quenching period, the first firing adopted a manually quenching by opening and closing the kiln door to realize the rapid cooling from highest temperature to lower than 600 degrees, while the second firing for hard coating samples were quenching automatically by the kiln controller. This operation intends to avoid crystallization zone, ranging from 780 degrees to 660 degrees, in which the glass has a higher possibility to crystalized. The avoidance of the crystallization aims at eliminates the structural influence results from it (Mukherjee & Das, 2016).

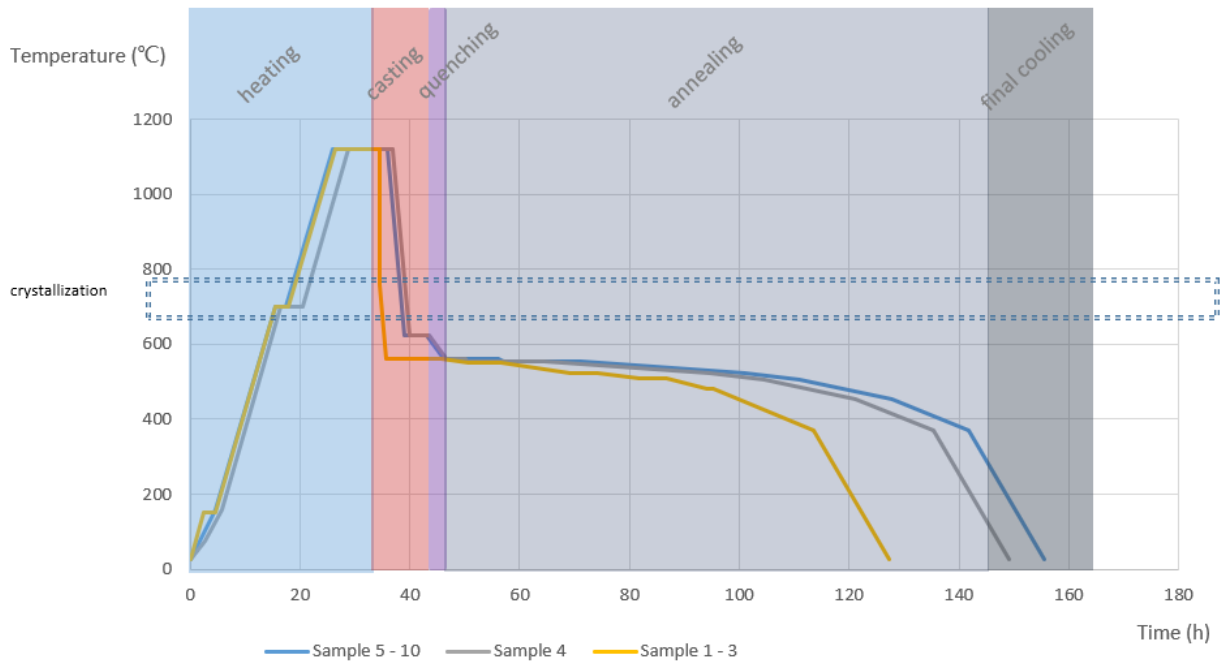


Fig. 3 The firing schedule for three kiln casting.

## 2.2. Recycled products and polarize observation

Fetches from the kiln, glass samples can be easily taken out of the crystalcast mould. As emerged in figure 4b), some lovely cell-shape trail shown in the top surface of the sample, which exposure to air during furnacing. Some operations should be taken for the samples, in order to prepare for the following tests. After the adjustment from cutting machine and grinder, the samples can be presented as a regular shape with smoother edges and flatter surface. The color of the final products is similar to each other, it is not easy to distinguish dark tints from light tints, which indicates there are no apparent appearance influence in float glass recycling result from the tints.

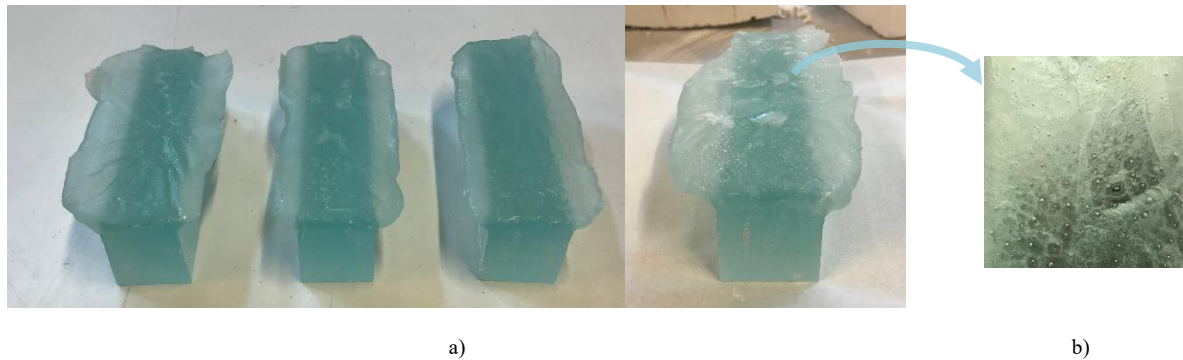


Fig. 4a) Samples after casting in a sequence from left to right: sample 3, sample 2, sample 1 and sample 4; b) a detailed look of the sample surface.

Due to the uneven distribution of temperature at the same time in the kiln-casting procedure of glass recycling, the temporary and residual stresses will appear, mostly developed in the annealing stage. After the manufacture, the products require quantitatively inspection on the residual stresses. As the result, integrating with the special transparent and birefringent properties of glass, an optical method based on photo-elasticity has been introduced. In the result of stress variation in the material, the refraction index of one specimen will vary in the different position of this specimen. When a polarized light passes through the photo-elastic material, the light will be disintegrated into different light beams due to the different indexes of refractive. Through these variations, integrating with stress-optic laws, the residual stress inside this specimen is able to be quantified (McKenzie & Hand, 2011).

For the recycled-glass samples in this experiment, it makes sense to exam the residual stress because of the considerable thickness. As the result, both plane polariscope and circular polariscope test are arranged for the samples. Figure 5 elaborating the patterns from plane polariscope test, in which the computer screen is chosen as a polarized light source. Along the edges through the height of the specimen, the patterns shown the trace of stress forming in the annealing period. It is formed by the varying temperature from surface to the central area of the specimen. However,

*The Application of Waste Float Glass, Recycled in Structural Beams made with the Glass Casting Method.*

these patterns are the combination results from isoclinic patterns and isochromatic patterns. To clarify the isochromatic lines and quantify the relationship between observation and stresses, the circular polariscope test has been introduced.

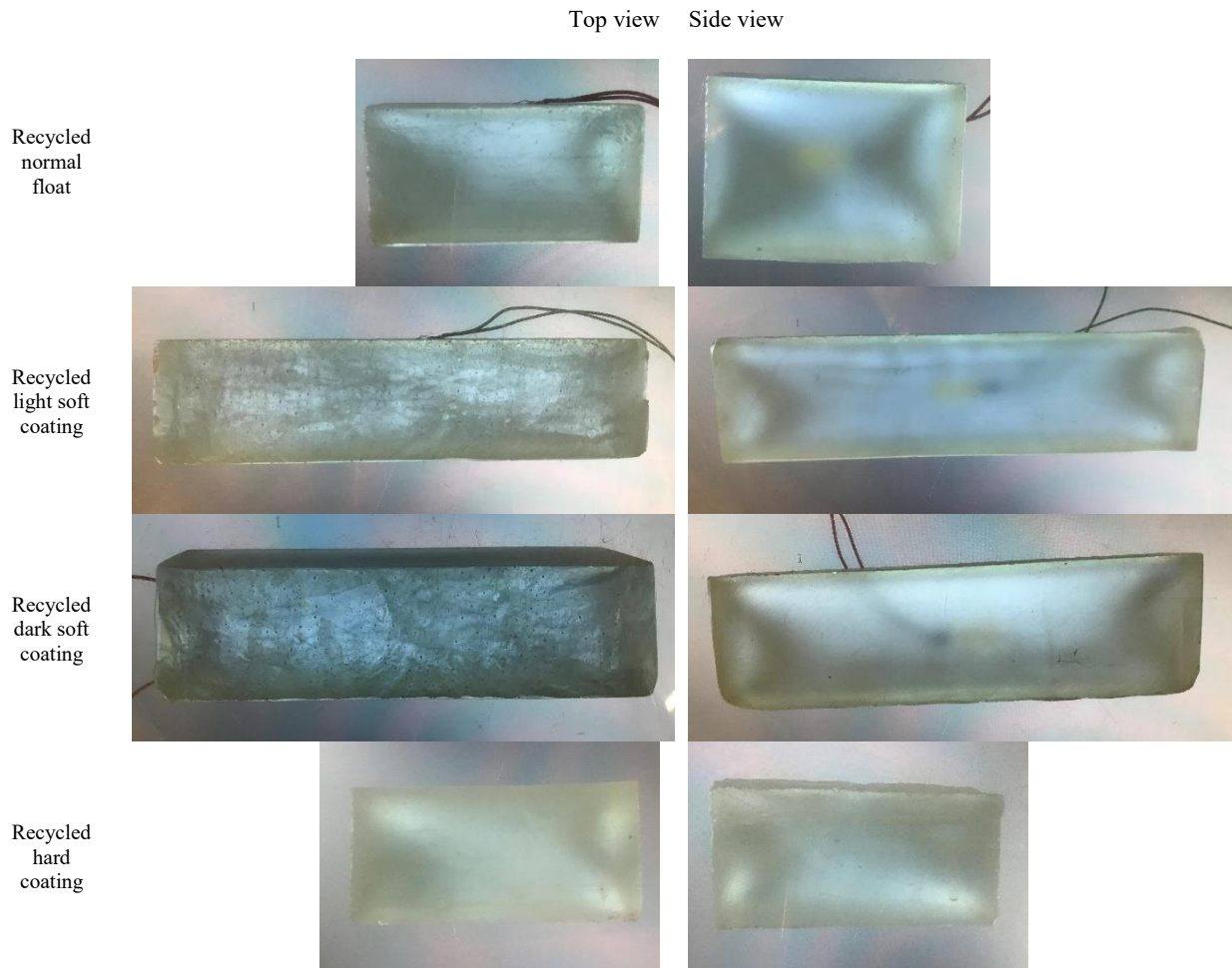


Fig. 5 The plane polariscope pictures (top view and side view) of sample 1 to 4, from top to bottom.

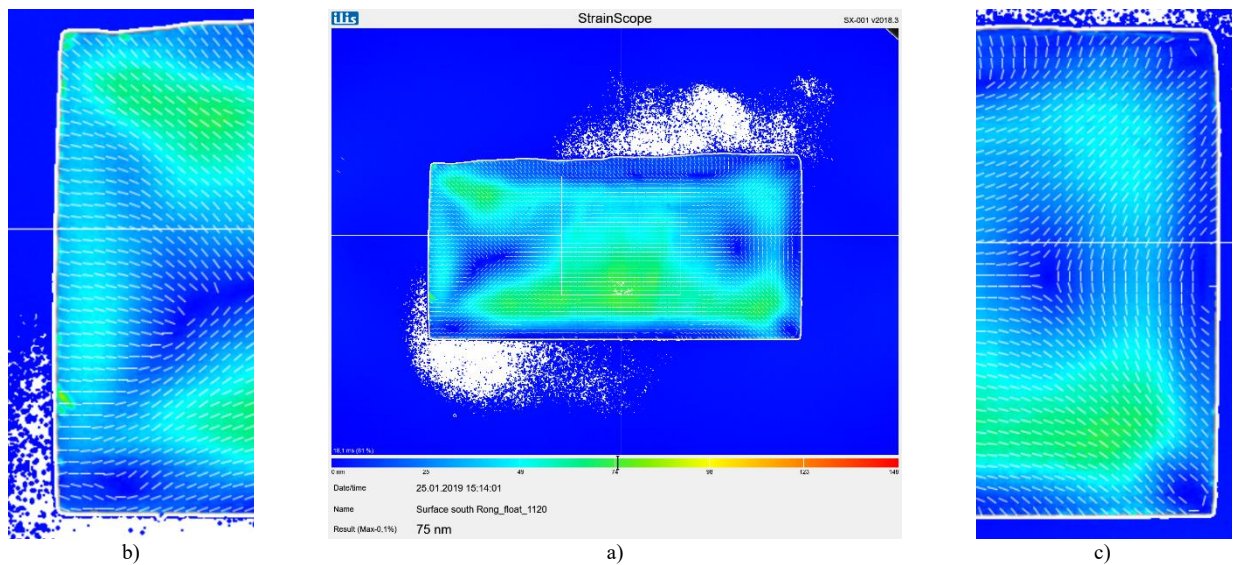


Fig. 6a) The output of normal float sample through circular polariscope test by Ilis, b) the detailed observation of sample's left part, and c) the detailed observation of sample's right part.

Thanks to the help of Ilis, a strain scope which can measure and image the mechanical stress of photo-elastic material expediently has been adopted. Limited by the time and expenditure, only one polished recycled glass specimen, which is half of the normal float sample with a cutting surface in left edge, are carried in this circular polariscope test. The

result exhibited in figure 6a. The direction of principal stress is drawn by the dash lines, and the dark blue area represented area without residual stress. Through the figure 6b, the direction of principal stress is perpendicular to the cutting surface, which can be regarded as the original orientation of the principal stress along the length of this specimen. The comparison is shown in the figure 7c, exhibiting a rainbow shape against the right edge, representing the surface attaching to the mould. This curved shape perfectly performing the formation of the internal stress during annealing. Meanwhile, the green area in the middle part of the specimen corresponding to the flowing of molten glass, owing to the different temperature in the mould. (Bristogianni et al., 2017).

Applying the thickness of 40mm and the photo-elastic coefficient of 2.7 TPa-1, the maximum residual stress is calculated as 0.69 MPa, which is relatively low as this stress are distributed along the thickness. By observing and calculating, the recycled float glass samples can be regarded as well-annealing and homogenous, based on the photo-elastic results.

### 2.3. XRF analysis

As illustrated before, to process further analysis and comparison, the chemical composition of original glass samples should be comprehended at first. This XRF test defined different chemical composition by different energy release, which is determined by characteristic of specific element. Conclude from the XRF test result, the chemical composition of four glass samples on both sides are presented in the following figure:

	Normal float glass		Soft coating (light)		Soft coating (dark)		hard coating	
	a	b	a	b	a	b	a	b
	tin bath		coated	tin bath	coated	tin bath	coated and tin bath	
SiO <sub>2</sub>	74.432	73.212	64.96	73.301	64.665	72.882	49.967	73.412
Na <sub>2</sub> O	12.524	12.453	4.765	12.483	4.736	12.714	0.577	12.086
SnO <sub>2</sub>		1.175	2.67	1.076	2.732	1.236	32.384	
CaO	8.23	8.397	8.969	8.406	9.253	8.45	14.241	9.063
MgO	3.884	3.797	2.318	3.778	2.273	3.83	1.153	4.262
Al <sub>2</sub> O <sub>3</sub>	0.55	0.577	0.506	0.571	0.549	0.52	0.317	0.561
K <sub>2</sub> O	0.145	0.135	0.16	0.139	0.16	0.134	0.453	0.295
SO <sub>3</sub>	0.113	0.14	0.097	0.125	0.171	0.112	0.237	0.144
Fe <sub>2</sub> O <sub>3</sub>	0.057	0.051	0.079	0.056	0.094	0.065	0.35	0.11
TiO <sub>2</sub>	0.029	0.028	0.294	0.025	0.364	0.022	0.154	
SrO	0.009	0.01	0.024	0.01	0.024	0.009		
P <sub>2</sub> O <sub>5</sub>	0.009	0.011	0.011		0.009	0.01	0.009	0.022
ZrO <sub>2</sub>	0.009	0.008	0.03	0.012		0.006	0.055	0.015
MnO	0.006	0.005	0.016	0.008	0.009	0.008		
ZnO	0.002	0.002	15.064		14.703	0.002	0.02	
Ag <sub>2</sub> O			0.03		0.04			
Au			0.007					
NiO					0.033			
Cr <sub>2</sub> O <sub>3</sub>					0.021			
Rb <sub>2</sub> O							0.013	
Cl							0.069	0.03

Fig. 7 The chemical composition content of original float glass.

The tin bath side can be distinguished depending on the content of tin, which is approximately 1% content. Referring to the coating side, it can be recognized based on the coating technology or the content of the tin dioxide. Through comparing the chemical constitution of tinted glass (light soft coating and dark soft coating glass) with the transparent glass (normal float glass and hard coating glass), the iron content is higher in former glass than later, corresponding to the green color given by ferric oxide. Besides, in comparison within the tinted glass, the dark soft coating has extra chromium oxide, which provide extra green for dark tints.

Except for the original float glass, the recycled glass has also taken for XRF test. At first, the surface for each recycled sample, which exposure to the air during furnacing, has taken for the XRF test. The result is shown in the figure below, with a relatively similar content of silica dioxide, which plays the major role in recycled samples. The leading chemical constitutions resulting in tints, such as ferric oxide, are unmeasurable after recycling. It corresponding to the statement that the amount of tints chemical is to small too affect the mechanical properties of the final products.

	SiO <sub>2</sub>	CaO	Na <sub>2</sub> O	MgO	Al <sub>2</sub> O <sub>3</sub>	SO <sub>3</sub>	K <sub>2</sub> O	Fe <sub>2</sub> O <sub>3</sub>	TiO <sub>2</sub>	Cl	MnO	SrO	ZnO	P <sub>2</sub> O <sub>5</sub>	ZrO <sub>2</sub>	Rb <sub>2</sub> O
Recycled normal float	89.973	6.354	2.115	0.94	0.3	0.118	0.075	0.117				0.009				
Recycled light soft coating	90.765	5.84	1.907	0.88	0.293	0.129	0.073	0.105				0.007				
Recycled dark soft coating	90.895	5.404	2.148	0.873	0.3	0.11	0.099	0.089	0.031	0.022	0.013	0.008	0.007			
Recycled hard coating	90.002	6.299	1.934	1.133	0.284		0.157	0.143		0.008		0.005		0.019	0.015	0.002

Fig. 8 The chemical composition content of surface from sample 1 to 4.

Owing to the extreme high amount of silica dioxide for the surface of all recycled samples, which may indicate a movement or exchange of the chemical content during casting, a further analysis has been applied in the different levels along the height of the samples. Restricted by the cost and time consumption, only recycled normal float glass sample and recycled hard coating glass sample are setting for the different-level XRF test. In figure 9, the normal float glass chemical composition before and after recycling are listed, as well as the constitution of hard coating glass.

Normal float glass						
	Normal float glass		Recycled normal float glass			
	Bare side	Tin side	Surface	Top	Middle	Bottom
SiO <sub>2</sub>	74.432	73.212	89.973	71.882	72.341	71.855
Na <sub>2</sub> O	12.524	12.453	2.115	12.883	12.545	13.052
CaO	8.23	8.397	6.354	9.93	9.861	9.74
MgO	3.884	3.797	0.94	4.051	3.959	4.069
SnO <sub>2</sub>		1.175				
Al <sub>2</sub> O <sub>3</sub>	0.55	0.577	0.3	0.593	0.558	0.649
SO <sub>3</sub>	0.113	0.14	0.118	0.295	0.374	0.344
K <sub>2</sub> O	0.145	0.135	0.075	0.166	0.169	0.171
Fe <sub>2</sub> O <sub>3</sub>	0.057	0.051	0.117	0.075	0.1	0.068
TiO <sub>2</sub>	0.029	0.028		0.036		
P <sub>2</sub> O <sub>5</sub>	0.009	0.011		0.016	0.018	0.009
SrO	0.009	0.01	0.009	0.011	0.009	0.01
ZrO <sub>2</sub>	0.009	0.008				
MnO	0.006	0.005				
ZnO	0.002	0.002			0.009	0.006
Cl				0.046	0.048	0.027
CuO				0.016	0.009	

a)

Hard coating glass						
	Hard coating		Recycled hard coating			
	Tin and coated side	Bare side	Surface	Top	Middle	Bottom
SiO <sub>2</sub>	49.967	73.412	90.002	73.011	73.167	73.405
Na <sub>2</sub> O	0.577	12.086	1.934	11.64	11.799	11.714
CaO	14.241	9.063	6.299	9.268	9.057	9.047
MgO	1.153	4.262	1.133	4.923	4.802	4.814
SnO <sub>2</sub>	32.384			0.024	0.054	
Al <sub>2</sub> O <sub>3</sub>	0.317	0.561	0.284	0.518	0.524	0.523
SO <sub>3</sub>	0.237	0.144		0.002		
K <sub>2</sub> O	0.453	0.295	0.157	0.364	0.394	0.331
Fe <sub>2</sub> O <sub>3</sub>	0.35	0.11	0.143	0.145	0.142	0.109
TiO <sub>2</sub>	0.154			0.03		
P <sub>2</sub> O <sub>5</sub>	0.009	0.022	0.019	0.029	0.021	0.021
SrO			0.005	0.003	0.003	0.004
ZrO <sub>2</sub>	0.055	0.015	0.015	0.016	0.016	0.015
ZnO	0.02			0.008		
Cl	0.069	0.03	0.008	0.018	0.007	0.018
Rb <sub>2</sub> O	0.013		0.002			

b)

Fig. 9a) The chemical composition content of sample 1 and b) for sample 4.

Normal float glass				
	surface	top	middle	bottom
SiO <sub>2</sub>	15.541	-2.55	-2.091	-2.577
Na <sub>2</sub> O	-10.409	0.359	0.021	0.528
CaO	-1.876	1.7	1.631	1.51
MgO	-2.944	0.167	0.075	0.185

a)

Hard coating glass				
	surface	top	middle	bottom
SiO <sub>2</sub>	16.59	-0.401	-0.245	-0.007
Na <sub>2</sub> O	-10.152	-0.446	-0.287	-0.372
CaO	-2.764	0.205	-0.006	-0.016
MgO	-3.129	0.661	0.54	0.552

b)

Fig. 10a) The differentials of dominate chemical compositions between sample 1 and bare side of original normal float glass and b) between sample 4 and bare side of original hard coating glass.

Through the comparison, an upward movement of silica dioxide can be easily noticed after casting in both samples. On the contrary, a clear alkali deposition along the height of sample 1 is shown. However, the alkali deposition is not that clear in the recycling process of hard coating glass. Besides, after recycling, the unfavourable chemical constitutes, tin (SnO<sub>2</sub>), becomes unmeasurable in the recycled normal float glass, but stays in a very low amount of hard coating glass. The influence from the constitution movement will be connected to the mechanical properties in the next chapter. The following test will be based on the XRF result of middle area, owing to the reliable content compare to the constitution before recycling.

### 3. Mechanical test and results

Referring to a common bending material, there are several essential properties in mechanical behavior, such as elastic modulus, coefficient of thermal expansion and fracture strength, which influence the deflection, bending capacity and

mechanical behavior under different temperatures. In this chapter, these three mechanical properties for recycled-float glass will be figured out through laboratorial test. The test results will be discussed and explained associating with chemical compositions.

### 3.1. Young's modulus test

- Methodology

Owing to the amount the samples (the load-displacement method and vibration method requires more samples in one category), the ultrasonic testing method has been chosen to test the Young's modulus of each samples. In order to meet the requirements of ultrasonic test, the side surface was polished in advance and applied with Vaseline on top. The testing process shows in figure below, on the screen of sound velocity detective equipment showing the time of sound travel through the lengthwise of the specimen, the same process will be carried to other four specimens as well.



Fig. 11 The ultrasonic method for Young's modulus testing, photo by author.

- Data collection

Despite of the time of flight from the ultrasonic devices, the dimension of four recycled glass specimens are also required, as well as the volume and the weight to derive the density. Except for simply measurement of dimension and weight, the volume was measured through the drainage method and corrected with the calculated results. The value of sound velocity is equals to the ratio of length in longitudinal direction to the time of flight. And the density is equals to weight divided by corresponding corrected volume. The corresponding data shows in following table:

Table 2: Young's Modulus calculation through ultrasonic method.

	Recycled normal float glass	Recycled light soft coating glass	Recycled dark soft coating glass	Recycled hard coating glass
Sound velocity [m/s]	5344.83	5000	5322.03	5293.10
Density [Kg/m <sup>3</sup> ]	2504.32	2531.30	2419.67	2399.28
Young's modulus [GPa]	71.54	63.28	68.53	67.22

- Analysis and discussion

Abstracting from A. Winkelmann and O.Schott's glass modeling (Zschimmer & Cable, 2013), the glass property can be calculated by the chemical composition integrated with corresponding coefficient. Through analyzing the relationship between glass properties and specific chemical composition, a prediction of glass behavior is able to be realized. Therefore, it is worthy to compare and analysis the correlation between Young's modulus and chemical composition of recycled float glass. In view of the glass database, theoretically, the relevancy of Young's Modulus and chemical constitution can be concluded as: a) the alumina plays the most important role in depending elasticity of glass, it improves Young's modulus by increasing the content; b) silica also improve the Young's modulus with a comparatively high coefficient; c) the content of metal oxide is in proportion to the value of Young's modulus; d) the alkali oxide will negatively affect glass elasticity; e) the content of alkali earth oxide is favor of modulus, while when the magnesia oxide takes the dominant place, the Young's modulus will be decreased.

### *The Application of Waste Float Glass, Recycled in Structural Beams made with the Glass Casting Method.*

The a) and b) are derived from Eberhard Zschimmer's book (Zschimmer & Cable, 2013), it gives the influence coefficient for alumina and silica of 130 to 180 and 70 respectively. The aluminum ion can fill the space in silica oxide structure, which give the glass structure more density, so that the glass can perform better in elasticity. Meanwhile, the silica oxide gives a strong bond in the structure, leading to a higher modulus. Besides, the conclusion c), d) and e) are obtained from Varshneya (Varshneya & Mauro, n.d.) and Kilinc & Hand (Kilinc & Hand, 2015). In general, the weaker the bond strength, the lower the Young's modulus. Correspondingly, the alkali will ruin the silica bond, which the alkali earth can worked as the modifiers to improve the bond strength. Depending on the theoretical database, the comparison existing in recycled float glass between Young's modulus and influential chemical compositions are presented in the chart below.

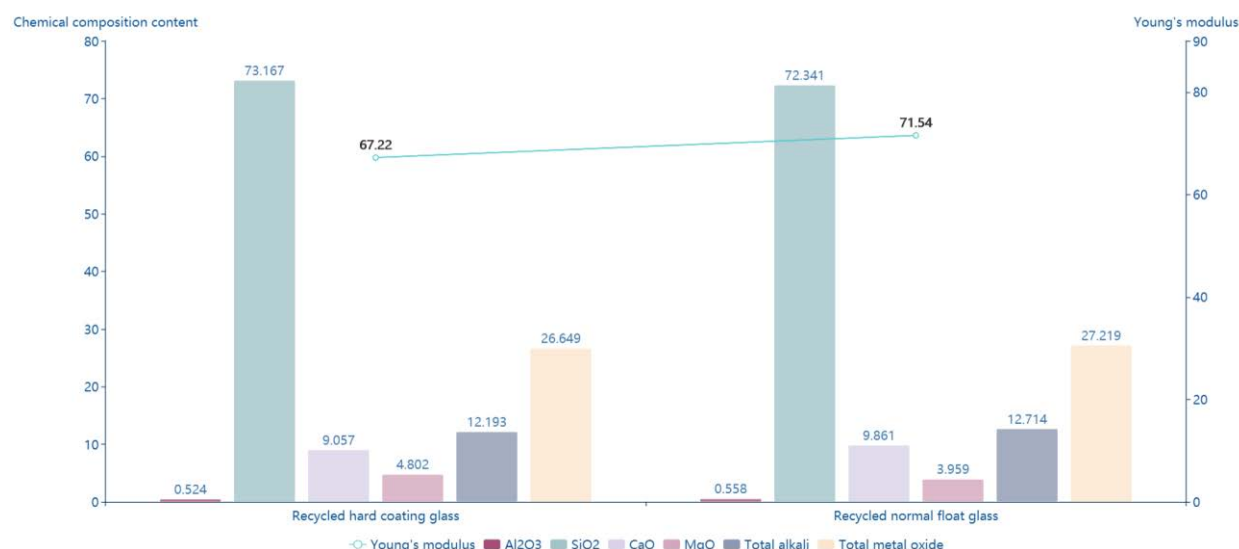


Fig. 12 The comparison in influential content of Young's modulus, between sample 1 and sample 4.

Because the ultrasonic test was applied to the side surface of the specimen and the sound were transfer in lengthwise. Thus, only the chemical compositions in the middle area of recycled hard coating glass and recycled normal float glass are taken to analysis. Referring to the chart above, although the recycled normal float glass has lower content in silica oxide, the higher aluminum oxide helps to fill the gap in the structure to increase the bond. In combination with the value of influential coefficient, the recycled normal float glass has a higher modulus. Also, the higher metal oxide content in recycled normal float glass corresponding to the higher Young's modulus. Considering the alkali earth element, the calcium oxide takes the dominant position in recycled normal float glass, which is nicely in consistence with the theory above.

However, the recycled hard coating glass has less alkali content than recycled normal float glass, which indicates less harm to the bond strength, but it has a lower Young's modulus. On the one hand, the disagreement may result from the various distribution of chemical composition along the height of the specimen, as well as the probable density variant in the specimen. On the other hand, this discrepancy can be a certification that the elasticity of glass cannot be decided by one category of influential chemical composition. It is possibly to conclude that it is difficult to predict Young's modulus based on one composition, since it depends on complex compositions integration with corresponding coefficients.

### *3.2. Coefficient of thermal expansion test*

#### ● Methodology

Basically, the measurement of CTE is the deformation measurement of the target material over the temperature range, in the goal of linear thermal expansion. Compare to other methods, the strain gauge methods have less restriction by applying strain gauges on the smooth surface of samples. However, the specific strain gauge and glue should be verified according to different temperature range. In view of practical work of recycled float glass, the temperature range of structural application should not exceed nature temperature. Hence, in this test, the temperature interval is set as ambient temperature to 80 degrees (176 °F).

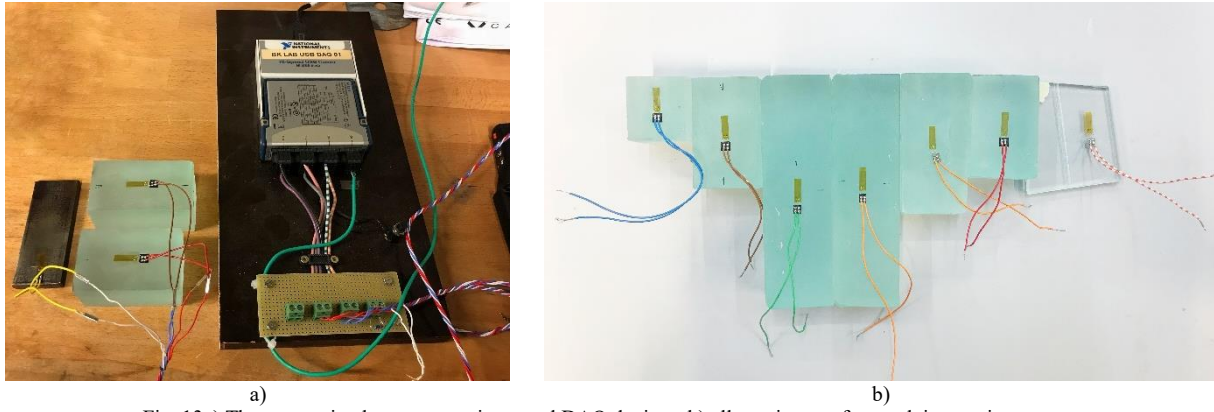


Fig. 13a) The connection between specimen and DAQ devices; b) all specimens after applying strain gauges.

Shown in the figure 13a is the connection among strain gauge, specimen and DAQ detector: the specimens' surface is attached with corresponding strain gauges, connecting through wires to the DAQ detector, which connected with three specimen and one temperature detector in one side, the other side is linked with computer. Among three specimens, stainless steel appears as a reference material, with a known CTE value of  $12 \mu \text{ m/m}^\circ\text{C}$ , while the others are prepared samples. After finishing all connection, the specimen will be put into the oven. All these tests share the same heating schedule: heating up to 80 degrees with a ramp of 200 degrees per hour and cooling down to the ambient temperature naturally.

#### ● Data collection

As alluded above, for each test, the receiver will collect four series of different information: the temperature change, the strain of two sample materials and the strain of reference material, all the data change over time. From the top chart in the screenshot, the temperature will remain in constant at the highest temperature for a period, and the strain of glass samples are continue increasing negatively. Since the specimen has a considerable thickness, it requires some time to adapt the heat. The period of constant temperature gives it time to stable itself. In total, seven tests have been finished, shown in order to withdraw a more authentic result, sample 1 (the recycled normal float glass) has been tested for five times, meanwhile the sample 4 (recycled hard coating glass) and original normal float glass specimens have been tested for three times. In the following analysis, the average result for each of these three categories will be selected for final calculation.

#### ● Analysis and discussion

Based on the theory of Wheatstone bridge for strain gauges, J. Valentich (Valentich, 1985) bring forward the equation to describe the value from strain gauge test. To gain the CTE value of the samples, the equation can be written as below:

$$\varepsilon' = (\alpha - \alpha_c) \Delta T \quad (1)$$

$\varepsilon'$ : Measured strain, micrometer per meter

$\alpha$ : CTE of samples

$\alpha_c$ : CTE of reference specimen

$\Delta T$ : Temperature variation in degree

In order to gain the CTE of the samples, the equation can be rewriting as below:

$$\alpha = \frac{\varepsilon'}{\Delta T} + \alpha_c$$

where:  $\varepsilon' = \varepsilon - \varepsilon_c$  (2)

The  $\varepsilon$  is the measured strain of samples and the  $\varepsilon_c$  is the measured strain of reference material, which are all obtained from the test. To enable the calculation, the negative information of recycled-glass samples will be regarded as positive results in the following analysis. Among all the data from tests, the strain value at initial temperature is taken as the

initial strain value, meanwhile the highest strain of samples is selected corresponding to the highest strain of stainless steel. The temperature variation will be calculated according to the strain value. After eliminating a set of inaccurate numbers, the rest 6 sets are included into calculation. The CTE value of stainless steel is selected as 12 in this calculation. As the strain gauge and tested samples are produced from different material, the measured strain in CTE test might be influenced by the deformation of strain gauges. Besides, the other parts of the correction come from the floating value of strain gauge electrical resistivity over temperature, it results from the strain gauge itself. To eliminate the influence, a definition called apparent strain is introduced, applying in correcting the result of CTE measurement. [32] It can be derived from the quadratic equation of thermal output as following:

$$\varepsilon_{app} = -2.27 \times 10 + 1.35 \times T - 1.07 \times 10^{-2} \times T^2 + 8.57 \times 10^{-6} \times T^3 + 1.70 \times 10^{-8} \times T^4 \quad (3)$$

The  $\varepsilon_{app}$  is the value of apparent strain, with a unit of micrometer per meter. And T is the on-time temperature with a unit of degrees. This equation can be obtained from the data sheet of strain gauge. Similarly, the strain gauge factor is also tested by the manufactures, as well as the strain gauge factor is regard as 2.01. To full fill the correction, an equation using apparent strain and strain gauge factor together to amend strain:

$$\varepsilon_{compensate} = (\varepsilon - \varepsilon_{app}) \times \beta \quad (4)$$

Where  $\beta$  is the value of gauge factor, which equals to 2.01 in this test. Combining with the electrical resistivity correction and thermal compensation correction, the final CTE values of all samples can be conclude as follows:

Table 3: CTE value of the sample 1 to 4.

	Original normal float glass	Recycled normal float glass	Recycled light soft coating glass	Recycled dark soft coating glass	Recycled hard coating glass
CTE value [ $\mu\text{m}/\text{m}^\circ\text{C}$ ]	5.736	5.529	5.315	5.805	5.473

The CTE value of glass are mainly influenced by the bond strength between metal cation and oxygen ion: for one thing the bigger ionic radius metal cation obtained, the weaker the bond will be; For another, the bond strength is proportional to the electrovalence of metal cation. Both a higher electrovalence and a smaller ionic radius means a higher chemical bond in metal oxide (White, 1976). Despite on the bond strength between metal cation and oxygen ion, among the metal oxide, the alkali and aluminum have special influence in glass thermal expansion. The alkali will increase the basicity, which will damage the bond of silica dioxide structures, so that the expansive prevention from silica will be weaken. In contrast, the aluminum can perform as a modifier which stronger the silica-oxygen bond, leading to less expansion. Based on the Schott's table (Zschimmer & Cable, 2013), the coefficient for sodium oxide and potassium oxide are 10 and 8.5 respectively, while a lower coefficient for aluminum is 5 in thermal expansion. Apart from the influence illustrates above, a strong chemical bonding exists between cation and anion in silicon-oxygen tetrahedron, which prevent expansion when temperature increasing, so that the higher the silica contained the less the CTE value will be (KARKHANAVALA & HUMMEL, 1952). However, the influence coefficient for silica is relatively low in Schott's table, which is 0.8. The silica will only be taken into consideration when it has a relatively high content in glass compositions.

For further investigations, the analysis goes deeper with the XRF results of the middle area of recycled normal float glass and recycled hard coating glass, as well as the bare side of original normal float glass. Extracting from figure 14, sample 1 has a slightly higher CTE value than sample 4, but lower than the CTE value of original float glass.

In between sample 1 and sample 4, the alkali content for the former is higher than the later, as well as the content of calcium oxide which will increase the expansion as the same as the function of alkali oxide. Even though the influence coefficient of silica for thermal expansion is inappreciable compared to alkali, it takes the dominate composition in soda lime glass, which may lower the CTE value. Consistent with this, the hard coating sample who has a higher amount of silica oxide own a lower CTE value. Despite the alkali and silicate, the calcium also helps expansion while the aluminum oxide prevents the expansion, both of them sit in the same level of CTE impact (Zschimmer & Cable, 2013). Owing to the relatively low weight content of aluminum, the influence of the higher amount may be eliminated by other chemical compositions. In general, the reliability of the test result for recycled glass is believable, and it is rational to demonstrate that the recycled hard coating glass has a lower CTE value than recycled normal float glass.

Nonetheless, through the comparison between original float glass and sample 1, the lower silicate content and higher alkali content for the recycled glass seems not able to grow the ability of expansion. Only the influence of aluminum is in consistence with the theory. This phenomenon can be explained by the uniform distribution of silicate and alkali in sample 1, the attaching area of strain gauge may have a higher silica and less alkali than original float glass. Hence,

it is not completely trustworthy to predict the CTE only from the chemical composition without experiment (Shelby, 2005).

Table 4: coefficient value of CTE.

	Na <sub>2</sub> O	K <sub>2</sub> O	CaO	Al <sub>2</sub> O <sub>3</sub>	SiO <sub>2</sub>	MgO
Coefficient	10	8.5	5	5	0.8	0.1

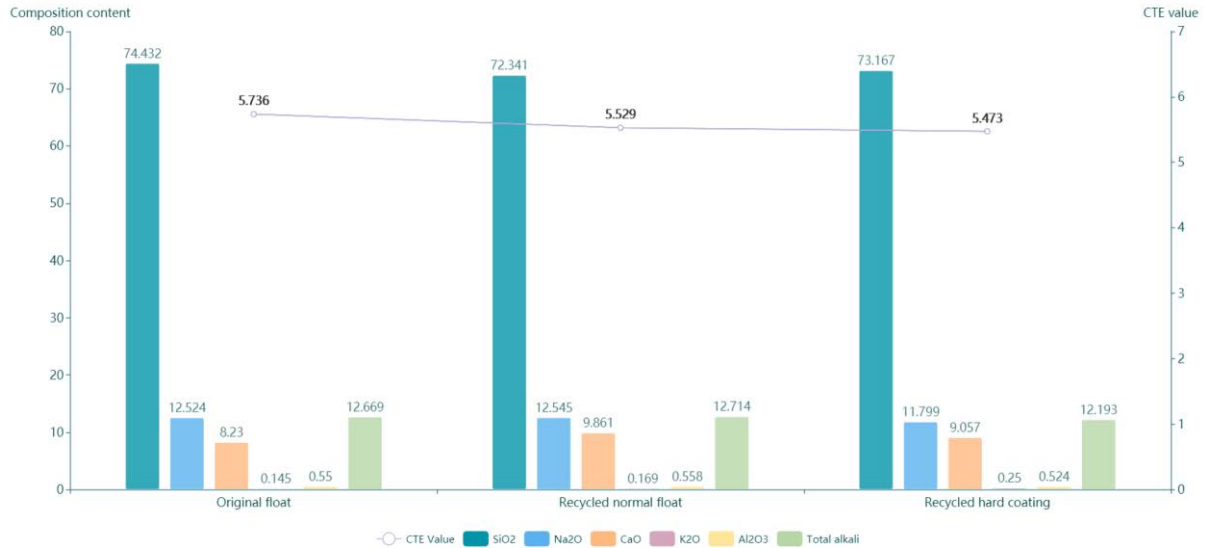


Fig. 14 The comparison of chemical composition content and CTE value, between original float glass, sample 1 and sample 4.

### 3.3. Fracture strength test

#### ● Methodology



Fig. 15 The four-point bending test for sample 5 to 10, photo by author.

$$\sigma_{\max} = \frac{M_c}{I} = \frac{3Pa}{bh^2} \quad (5)$$

$\sigma_{\max}$ : The flexural stress in correspond to break force;

b: The width of the specimen;

h: The height of the specimen;

P: The loading force;

a: The distance between loading point and supporting point.

### *The Application of Waste Float Glass, Recycled in Structural Beams made with the Glass Casting Method.*

For brittle materials such as ceramics or glass, a three-point bending or four-point bending test are usually adopted to measure the tensile strength. Integrating with the dimension of sample specimens and the stability during loading, a 1/4 point four-point bending test ( $a=L_0/4$ ) has been selected,  $a$  is the moment arm while  $L_0$  is outer span length. Sample 5 to 10 in dimension 2 have been prepared for testing, all of them are recycled from the mixture of coated glass. Owing to the limit thickness of the beam, the polishing can only be processed to the edges of each sample. Besides, the “stand up” test required extra supporting system, which may introduce uncertainties to the test. Thus, this four-point bending test will be proceeded in a horizontal direction, a “lay down” position, presented in figure 15. The loading rate has been programmed as 1 millimeter per minute, and the software will record the load, derived from the loading point, and the displacement at the same location. Depending on the break load and maximum load, the corresponding stress can be derived (Hertzberg et al., 2013).

#### ● Data collection

After loading, the corresponding load and displacement results were recorded computationally. To visualize the result, the data has been graphing in figure 16, with obvious similar trending for all glass samples. The small curve in the beginning period result from the adaption of the bending equipment, then the curve transfer into a linear phase until the broken point. Obtaining from the data, the maximum displacement is 0.65mm obtained by sample 5 and the maximum break strength among this samples is 880.968 N from sample 6. All the beams are broken in the tension zone, shown in figure 17, as primary evidence of the failure caused by bending.

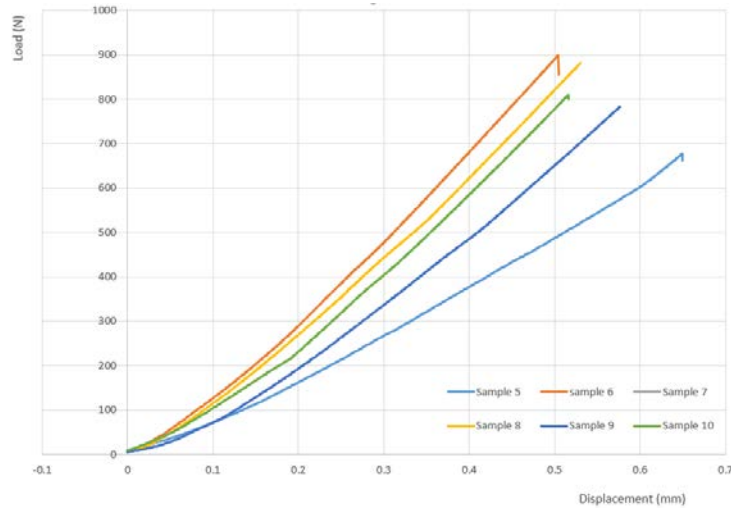


Fig. 16 The load-displacement curve for sample 5 to 10.

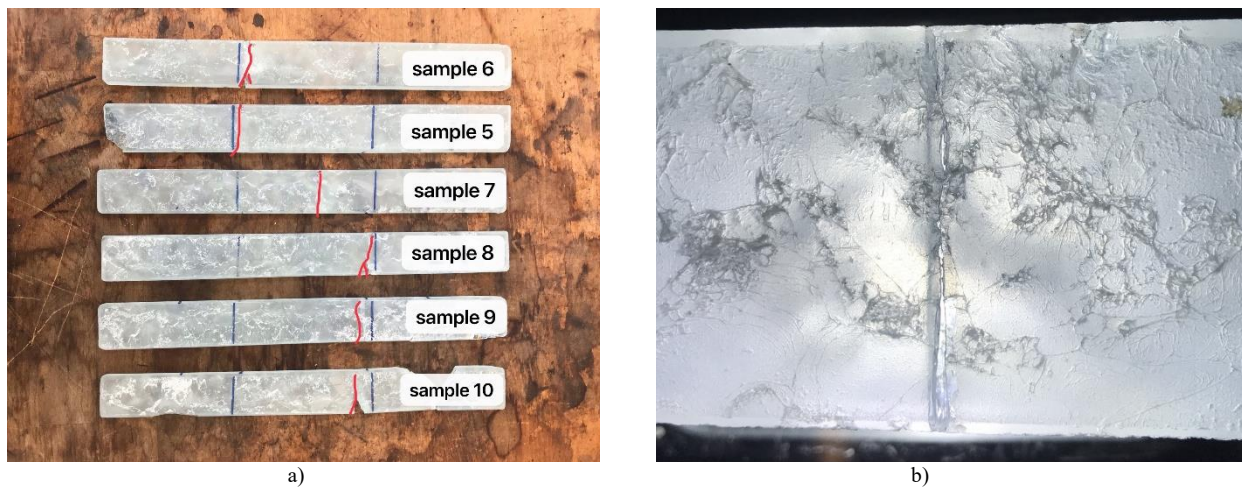


Fig. 17a) The dominate crack for sample 5 to 10; b) the detailed flaws in the surface of sample 7.

Build on the data above, the authors assume this recycled glass material is homogeneous in order to use the simple beam theory. Therefore, the flexural stress under break load can be calculated as an average value of  $25.64\text{N/mm}^2$ , which is lower than the flexural stress of original float glass (assigned as  $41\text{N/mm}^2$  from NSG group). Besides, the magnitude of Young's modulus can be speculated from the load-displacement curve, since the curvature of load-

displacement curve is the stiffness of recycled glass, which is in proportional of Young's modulus. Therefore, except for sample 5 and sample 10, the other samples have very similar Young's modulus.

#### ● Fracture analysis

To identify the breakage mechanism and the cause of failure, the analysis of fracture surface is investigated with microscope (VHX-700 Digital Microscope), assisted by the visual study of the sample surface. Through this analysis, the decreased flexural strength of the recycled glass material could also be speculated. The sample 5 and sample 8 are taken to be analyzed, shown in the following figures.

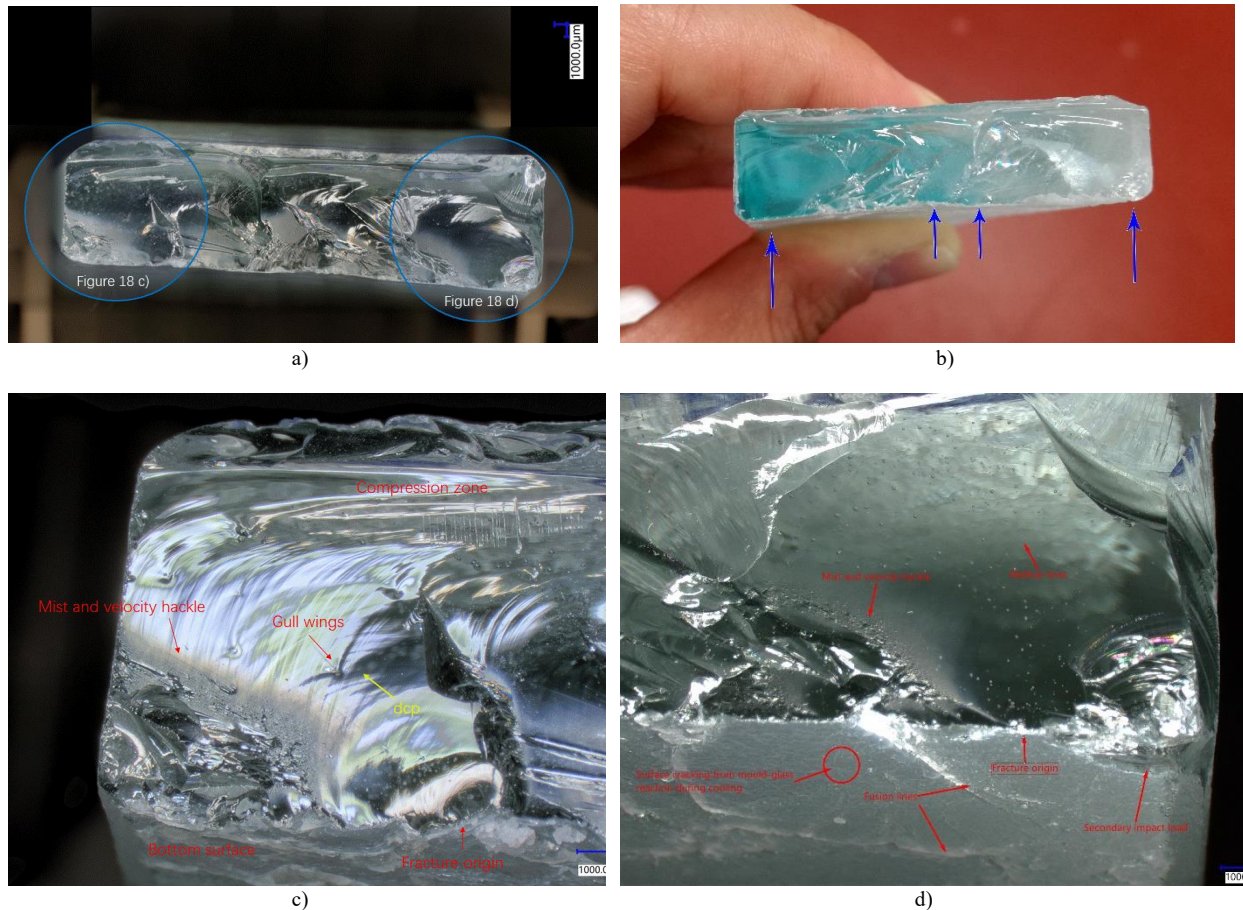


Fig. 18a) The microscope observed fracture surface of sample 5; b) the opposite fracture surface of sample 5; c) a detailed observation of sample's left part; d) a detailed observation of sample's right part.

According to the generally observation, there are multiple fracture mirrors (at least 4 fracture mirrors appointed in figure 18b)) appeared in the fracture surface. The detailed images were captured for two bigger fracture mirrors, locates in left and right corner or fracture surface. In figure 18c), according to the Wallner lines and velocity hackle the direction of crack propagation was found, from the fracture origin to the left upper corner, exhibit a transformation from bending to compression. Several gull wings appeared when the Wallner lines met the bubbles. In the meantime, the crack propagation was stopped by another fracture mirror on the right hand, confirming the existence of multiple fracture origins. These multiple fracture mirrors and the diameter of fracture mirrors indicating a lower energy consumption as well as lower stress (Ono & Allaire, 2000). The observation from part of the bottom surface and the fracture surface of right part (figure 18d)), showing another fracture mirror origin from the crystallized surface. The fusion lines and micro cracks exist obviously in the bottom surface, as the surface reaction to the mould during annealing process.

Similarly, a very thin layer of crystalline formation shown in the bottom surface of sample 8, in figure 19. A clear fracture mirror origin from the surface stone, meanwhile some sub cracks appeared due to the minor surface flaws. It demonstrated that the flexural strength will be influenced by the perfection of sample surface. Based on the experience from sample 1 to sample 4, the surface quality can be improved by simply polish this thin layer of crystallized interface.

Due to the lack of inter layer between bending machine and recycled glass specimen, the beam is directly stressed by bending roller, which may introduce stress concentration in the loading position, such as the right upper corner in

figure 19. Besides, these samples are tested with four-point bending fixtures in a displacement controlled universal testing machine, which not allowed for the minor adjustment. The error might happens owing to this articulation, which can explain the phenomenon that the crack appears close to one of the loading positions (Mitchell et al., 2009).

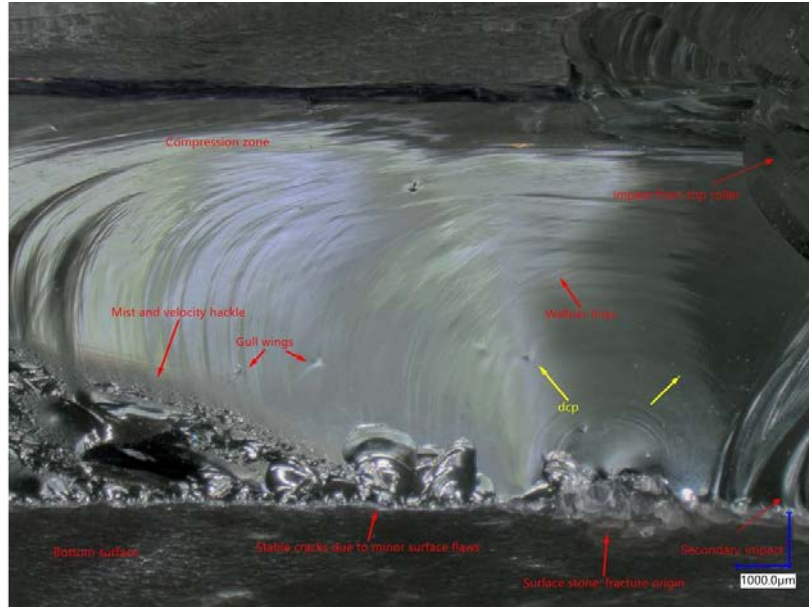


Fig. 19 The microscope images of the fracture surface of sample 8.

#### 4. Conclusion and further expectation

Through the cast experiments, mechanical tests and FEM analysis, this paper evaluated that the waste float glass can be recycled as a structural component with kiln-casting methodology under lower energy consumption, explaining as followed conclusions: a) Integrating with proper firing schedule, the sample 1 to 4 exhibit as the well-cast homogenized final products, proving that the coated float glass can be well-recycled as separate categories; b) Comparing sample 1 and 4 to sample 2 and 3, the color is indistinguishable, with the help of XRF test results, the chemical constitution who endow the tints in glass only taken a very small portion. Therefore, it is rational to conclude that the influence of recycled float glass from tints is neglectable; c) Through the microscope image of the fracture surface, only a very thin crystallized layer exists in the surface (owing to the mould reaction), the material inside is homogeneous. As the result, the coated float glass is possible to be recycled without sorting from different coating types; d) According to the ultrasonic test results, the recycling process through kiln casting will not decrease Young's modulus significantly. Like normal glass, the Young's modulus of recycled float glass can be regarded as a great advantage in the structural application as well; e) Similarly, comparing the CTE value of original normal float glass and recycled normal float glass (sample 1), the kiln-cast recycling will not have a negative influence in CTE value of float glass, deriving from the strain gauge test results; f) Combining with the XRF analysis, the impact (for both Young's modulus and CTE value) from chemical constitution should be integrated with corresponding influence coefficient and proportion. To conclude, the structural property of recycled float glass does not have substantial drawbacks, supported with the data in following table. Thus, a path to evaluate the recycling possibility of glass as a structural component is provided.

Table 9: The main structural properties for recycled float glass.

Young's modulus	Density	CTE value (25 – 80 °C)	Fracture strength	Flexural stress
[MPa]	[Kg/m <sup>3</sup> ]	[µm/ m°C]	[N]	[N/mm <sup>2</sup> ]
66345.9	2485.1	5.53	≥791.53	≥25.64

However, this path could be progressed in several aspects: in this flexural test, the initial flaws and crystallizations from the surface lead to a lower fracture strength. An improved bending system with allowance of adjustment or rotation at loading positions should be provided for the further investigation. To upgrade the surface condition, the dimension of the specimen should be optimized. Moreover, considering the good polarized result of dimension 1 compare to dimension 2, the recycled float glass can be used as volumetric structural elements, which could also apply in assembly of structural beams or columns. What's more, depending on the XRF test, the silica dioxide content of surface of sample 1 to 3 is extremely high, even more than 90%. It can be considered for the application in super high

compression conditions or thermal resistance glass surface; however, the thickness of this high-silicate surface must be defined beforehand. This paper only focused on float glass from one company, which has the very similar dominant chemical composition. In consideration of the difficulties of waste glass sorting, it is meaningful to recycled from mixtures of different glass brand, as well as find recycling possibilities in other glass types. Taken industrial application into consideration, the exact melting and softening temperature in this recycling process need to be clarified, in order to get the optimal energy-saving solution.

## Acknowledgements

The authors would like to express great appreciate to Martijn Rietveld from Pilkington for the resource support, Kouchi Zhang for the valuable suggestions, Ilis for providing StrainScope Flex, Ruud Hendrikx for the kind help in XRF tests, Albert Bosman for the supporting in Young's modulus test, Clarissa Justino de Lima and Paul Vermeulen for the helpful advice and help in CTE test, Tomasso Venturini and Kees Baardolf for the friendly help in lab work.

## References

- Bristogianni, T., Oikonomopoulou, F., de Lima, C. J., Veer, F. A., Nijssse, R.: Cast glass components out of recycled glass: Potential and limitations of upgrading waste to load-bearing structures. *Challenging Glass 6: Conference on Architectural and Structural Applications of Glass, CGC 2018 - Proceedings*, 6, 151–174 (2018). <https://doi.org/10.7480/cgc.6.2130>
- Bristogianni, T., Oikonomopoulou, F., Veer, F. A., Nijssse, R.: Production and Testing of Kiln-cast Glass Components for an Interlocking, Dry-assembled Transparent Bridge (2017) Coating Technology - Processes. (n.d.).
- Glass Coating Technology Comparison | Stewart Engineers. (n.d.). Retrieved March 31, 2020, from <https://stewartengineers.com/en/innovations/glass-coating-technology-comparison/>
- Hertzberg, R. W., P.Vinci, R., Hertzberg, J. L.: *Deformation and Fracture Mechanics of Engineering Materials* (2013). [www.iran-mavad.com](http://www.iran-mavad.com)
- Karkhanavala, M. D., Hummel, F. A.: Thermal Expansion of Some Simple Glasses. *J. Am. Ceram. Soc.* 35(9), 215–219 (1952). <https://doi.org/10.1111/j.1151-2916.1952.tb13105.x>
- Kilinc, E., Hand, R. J.: Mechanical properties of soda-lime-silica glasses with varying alkaline earth contents. *J. Non-Cryst. Solids* 429, 190–197 (2015). <https://doi.org/10.1016/j.jnoncrysol.2015.08.013>
- McKenzie, H. W., Hand, R. J.: *Basic Optical Stress Measurement in Glass*. Society of Glass Technology, Sheffield (2011)
- Mitchell, M. R., Link, R. E., Quinn, G. D., Sparenberg, B. T., Koshy, P., Ives, L. K., Jahanmir, S., & Arola, D. D.: Flexural Strength of Ceramic and Glass Rods. *J. Test. Eval.* 37(3), 101649 (2009). <https://doi.org/10.1520/jte101649>
- Mukherjee, D. P., Das, S. K.: Influence of TiO<sub>2</sub> content on the crystallization and microstructure of machinable glass-ceramics. *J. Asian Ceram. Soc.* 4(1), 55–60 (2016). <https://doi.org/10.1016/j.jascer.2015.11.004>
- Oikonomopoulou, F., Bristogianni, T., Barou, L., Jacobs, E., Frigo, G., Veer, F. A., Nijssse, R.: A novel, demountable structural glass system out of dry-assembly, interlocking cast glass components. *Challenging Glass 6: Conference on Architectural and Structural Applications of Glass, CGC (2018) - Proceedings*, May, 11–26. <https://doi.org/10.7480/cgc.6.2118>
- Ono, T., Allaire, R.: Fracture Analysis, A Basic Tool to Solve Breakage Issues. Taiwan FPD Expo (2000) November, 1–9. <http://www.new.corning.com/assets/0/391/2423/2437/2441/38FCE344-211C-454E-878C-2BD1A9105453.pdf>
- Shelby, J. E.: Introduction to Glass Science and Technology 2nd Edition (2005). In Book. [https://doi.org/10.1002/1521-3773\(20010316\)40:6<9823::AID-ANIE9823>3.3.CO;2-C](https://doi.org/10.1002/1521-3773(20010316)40:6<9823::AID-ANIE9823>3.3.CO;2-C)
- Silva, R. V., de Brito, J., Lye, C. Q., Dhir, R. K.: The role of glass waste in the production of ceramic-based products and other applications: A review. *J. Cleaner Prod.* 167, 346–364 (2017). <https://doi.org/10.1016/j.jclepro.2017.08.185>
- Valentich, J.: Thermal expansion of solids from -261°C to 173°C using strain gauges. *Cryog.* 25(2), 63–67 (1985). [https://doi.org/10.1016/0011-2275\(85\)90105-5](https://doi.org/10.1016/0011-2275(85)90105-5)
- Varshneya, A. K., Mauro, J. C. (n.d.). *Fundamentals of inorganic glasses*.
- Vieitez, E. R., Eder, P., Villanueva, A., Saveyn, H., Rodriguez Vieitez, E., Eder, P., Villaneuva Krzyzaniak, A., Saveyn, H.: End-of-Waste Criteria for Glass Cullet: Technical Proposals. In *Scientific and Technical Reports (Issue 1)* (2011). <https://doi.org/dx.doi.org/10.2791/7150>
- White, G. K.: Thermal expansion at low temperatures of glass-ceramics and glasses. *Cryogenics*, 16(8), 487–490 (1976). [https://doi.org/10.1016/0011-2275\(76\)90007-2](https://doi.org/10.1016/0011-2275(76)90007-2)
- Zschimmer, E., Cable, M.: *Chemical technology of glass* (2013).



Challenging Glass 7  
Conference on Architectural and Structural Applications of Glass  
Belis, Bos & Louter (Eds.), Ghent University, September 2020.  
ISBN 978-94-6366-296-3, [www.challengingglass.com](http://www.challengingglass.com)



#### PLATINUM SPONSORS

---



#### GOLD SPONSORS

---



#### SILVER SPONSORS

---



#### ORGANISING PARTNERS

---

